2008

Determination of Photochemically Produced Carbon Dioxide in Seawater

Emily M. White

David J. Kieber

Kenneth Mopper
Old Dominion University, kmopper@odu.edu

Original Publication Citation

White, E. M., Kieber, D. J., & Mopper, K. (2008). Determination of photochemically produced carbon dioxide in seawater. *Limnology and Oceanography: Methods, 6*, 441-453. doi:10.4319/lom.2008.6.441

LIMNOLOGY
and
OCEANOGRAPHY: METHODS

Limnol. Oceanogr.: Methods 6, 2008, 441–453

Determination of photochemically produced carbon dioxide in seawater

Emily M. White[1] , David J. Kieber[1], and Kenneth Mopper[2]*
[1]Department of Chemistry, State University of New York, College of Environmental Science and Forestry, Syracuse, NY 13210
[2]Department of Chemistry and Biochemistry, Old Dominion University, Norfolk, VA 23529

Abstract

An analytical system was developed to determine photochemically produced carbon dioxide in marine waters. Our system was designed to measure low levels of carbon dioxide by maintaining a closed system to prevent atmospheric contamination during sample preparation, irradiation, and analysis. To detect low levels of photoproduced carbon dioxide in seawater, background dissolved inorganic carbon (DIC) was removed before irradiation. To strip out DIC, samples were acidified to pH 3.0 (converting DIC to carbon dioxide) and bubbled with low carbon dioxide air. The pH was then readjusted back to the original value, and the resulting low-DIC seawater samples were transferred pneumatically to air-tight quartz tubes for irradiation. During analysis, samples were pneumatically transferred to a sample loop, injected, and acidified. Carbon dioxide was then stripped out, dried, and carried to a nondispersive infrared carbon dioxide analyzer. Calibration was done with a series of low concentration aqueous carbonate standards (0.05 to 3 μmol L^{-1}). The detection limit, defined as the concentration corresponding to three times the standard deviation of the experimental blank (i.e., DIC-stripped seawater), was ~60 nmol L^{-1}. Method precision was largely dependent on the agreement between multiple injections from the same tube (< ±2% relative standard deviation [RSD]) and the reproducibility between different tubes (±3% RSD). This method was used to measure carbon dioxide photoproduction in a variety of waters (e.g., estuarine, lake) including the first direct measurements in marine waters.

Introduction

Direct photochemical mineralization of dissolved organic matter (DOM) to carbon dioxide (CO_2) is an important removal pathway for terrestrial dissolved organic carbon (DOC) in coastal surface waters (Miller and Zepp 1995). Initial estimates for the global oceanic flux of photoproduced CO_2 range from 3 to 16 Pg C y^{-1} (Moran and Zepp 1997; Mopper and Kieber 2000). These values are based on flux estimates for photochemical carbon monoxide (CO) production (0.13 to 0.82 Pg C y^{-1}; Conrad et al. 1982; Valentine and Zepp 1993; Moran and Zepp 1997), assuming that CO_2 photoproduction is twenty times larger than CO photoproduction (Miller and Zepp 1995). Recent modeling studies suggest a smaller CO flux (0.05 Pg C y^{-1}; Zafiriou et al. 2003*a*; Stubbins et al. 2006), thereby reducing the estimate for photoproduced CO_2 to 1 Pg C y^{-1}. Although it is clear that direct photochemical oxidation is significant compared with the input of riverine DOC to the ocean (0.25 Pg C y^{-1}; Hedges et al. 1997), accurate quantification of this flux is needed to fully understand the role of photochemistry in the marine carbon cycle.

CO_2 photoproduction has been studied in freshwater systems (Miles and Brezonik 1981; Salonen and Vähätalo 1994; Miller and Zepp 1995; Granéli et al. 1996; Granéli et al. 1998; Moore 1999; Bertilsson and Tranvik 2000; Vähätalo et al. 2000; Anesio and Granéli 2003; Ma and Green 2004). However, coastal (Miller and Zepp 1995; Johannessen and Miller 2001; White et al. 2003; Bélanger et al. 2006; Skalski 2006; Johannessen et al. 2007) and open ocean water (Johannessen and Miller 2001; Kieber et al. 2003) studies are limited. This is primarily due to the analytical challenge of detecting low levels

*Corresponding author: E-mail: djkieber@esf.edu

Acknowledgments

We thank George Westby, Danielle Benati, Shannon Reilly, Lydia Bell, John Bisgrove, Don Haggart, Greg Nederveld, Adam Baumann, Kim Pierce, Jingnan Lu, Sara Button, Dr. Jane Sherrard, and the captain and crew of the R/V *Endeavor* for their assistance. We would like to express our appreciation to Dr. Oliver Zafiriou and Dr. Wei Wang for providing their isotopic exchange results and working with us on the comparison study. This material is based upon work supported by the National Science Foundation Chemical Oceanography Program (OCE-9711206 and OCE-0096426, KM; OCE-9711174 and OCE-0096413, DJK). Any opinions, findings, and conclusions or recommendations expressed in this material are those of the authors and do not necessarily reflect the views of the National Science Foundation. This work was also supported by NASA Headquarters under the Earth System Science Fellowship Grant (NGT5-30431, EMW).

of photoproduced CO_2 (~ nmol L^{-1}) above the high background of dissolved inorganic carbon (DIC) in seawater (~2 mmol L^{-1}). Based on reported rates of CO photoproduction of ~1 nmol L^{-1} h^{-1} (Kieber et al. 2003) and assuming CO_2 photoproduction is twenty times larger than CO photoproduction (Miller and Zepp 1995), photochemical CO_2 production rates are expected to be less than 0.2 μmol L^{-1} d^{-1} in open ocean water. To detect such a small change in DIC concentration relative to ambient DIC, a method with better than 0.003% precision is required (i.e., three standard deviations must be less than 0.2 μmol L^{-1}). More realistically, precision of better than 0.001% would be needed (based on a limit of quantification of 10 times the standard deviation).

The precision of commercially available systems is inadequate to measure CO_2 photoproduction in seawater (e.g., Shimadzu reports a precision of 0.3% for seawater with the TOC-5000; Application Note TOC-002). Better precision (0.075%) is achieved with the coulometric SOMMA system (Johnson et al. 1993) with modifications improving precision to 0.02% to 0.06% (Robinson and Williams 1991; Goyet and Hacker 1992). A comparable system with a non-dispersive infrared detector has also been developed with a reported precision of 0.05% (Kaltin et al. 2005). Given this limited precision, none of these methods are suitable for the direct determination of CO_2 photoproduction in seawater. The DIC must be stripped out of seawater before irradiation to detect low concentrations of photoproduced CO_2. However, under these conditions atmospheric contamination becomes a major concern (e.g., pure water in equilibrium with the atmosphere contains ~12 μmol L^{-1} CO_2).

This DIC removal approach was used to determine CO_2 photoproduction rates in water from the Mississippi River Plume (Miller and Zepp 1995) and apparent quantum yield (AQY) spectra in a number of estuarine (Bélanger et al. 2006; Skalski 2006), coastal (Johannessen and Miller 2001; Bélanger et al. 2006; Johannessen et al. 2007), and open ocean (Johannessen and Miller 2001) waters. AQY spectra were used to calculate a global annual oceanic CO_2 photoproduction flux of ~12 Pg C y^{-1} (Johannessen 2000). However, none of these studies have directly determined CO_2 photoproduction rates in marine waters.

This article describes a DIC analyzer and experimental procedure that were developed to precisely determine low levels of CO_2 photoproduction directly in marine waters. A lower limit of detection and improved precision are achieved by maintaining a closed system during sample preparation, irradiation, and analysis. Such measurements are needed to quantify the contribution of CO_2 photoproduction to the marine carbon cycle.

Materials and procedures

Chemicals—All chemicals were purchased commercially and used without additional purification. HPLC grade methanol and acetonitrile were purchased from Burdick & Jackson. Hexanes (GC Resolv), 85% o-phosphoric acid (certified ACS), 50% sodium hydroxide (certified), magnesium perchlorate (reagent grade anhydrous dessicant), and NIST-certified pH buffers were purchased from Fisher Scientific. Calcium oxide, Drierite (8 mesh), Ascarite(II), and 50% hydrofluoric acid were purchased from ACROS. Hydrochloric acid (ACS grade) used for routine glass cleaning and chloroform (HPLC grade) were purchased from EM Science. Hydrochloric acid (Ultrex II) was purchased from J.T. Baker. Indicating soda lime was obtained from LI-COR and phosphorus pentoxide desiccant was purchased from Fluka. Sodium carbonate was obtained from Shimadzu Corporation. Nitrogen (UHP) and a certified CO_2 standard (100 ppm in air) were purchased from Haun Welding Supply (Syracuse, New York). Clean, low-CO_2 (<1 ppm) air was produced from in-house compressed air using a Parker Balston 75-45 FT-IR Purge Gas Generator (Parker Hannifin). Nitrogen and air were passed through a column of Ascarite before use to remove any residual CO_2. Hi-EFF type 316 grade stainless steel tubing (1/8" OD, 0.085" ID, Alltech) was used for all gas lines. A Milli-Q ultrapure water system (Millipore) was used to obtain high purity laboratory water with a resistivity greater than 18 MΩ·cm. All glassware was cleaned by alternating rinses of water, and methanol, aqueous hydrofluoric acid (5%), and aqueous hydrochloric acid (10%), followed by baking at 400°C for 6 h.

Sample preparation—Marine samples were collected from the R/V *Endeavor* during the summer of 2002 (EN372) and 2003 (EN384) using 10 L GO-FLO bottles (General Oceanics) attached to a CTD rosette sampler (Sea-Bird Electronics). During the 2003 cruise, a sample was obtained at a depth of ~5 m from the ship's underway sampling system in the Cape Fear Estuary. Grab samples were also collected from Green Lake (Fayetteville, New York, USA). Samples were gravity-filtered through precleaned 0.2 μm nylon POLYCAP AS/HD filters (Whatman) into glass Qorpak© (All-Pak) bottles. Filter capsules were cleaned before use by alternating rinses of acetonitrile and Milli-Q water, followed by extensive flushing with Milli-Q water until no residual organic carbon was detected (by total organic carbon analysis). Samples not used immediately were stored in the dark at 4°C and refiltered into glass sparging bottles before use.

Sparging bottles (Fig. 1A) were made from 5 L Pyrex® media bottles (Corning) by attaching a Chem-Thread (13 mm OD, Chemglass) for use as a side port and a nylon sparging cap (drilled with three 1/4-28 holes). The sparging system consisted of a 2 μm PEEK bottom-of-the-bottle filter (Upchurch Scientific). FEP tubing (1/8" OD and 1/16" ID, Cole-Parmer) was fit to the cap holes with flangeless nuts and ferrules (Upchurch), as sparging and sampling lines. A drilled-out female luer adapter (1/4-28 ETFE, Upchurch) in the third hole of the cap was used as a vent that could be closed with a polypropylene male luer plug (Cole-Parmer). The cap was sealed to the bottle with Teflon tape to ensure a tight connection, and the sample was introduced through the side port. This side port also allowed for the insertion of a pH electrode (FUTURA refillable

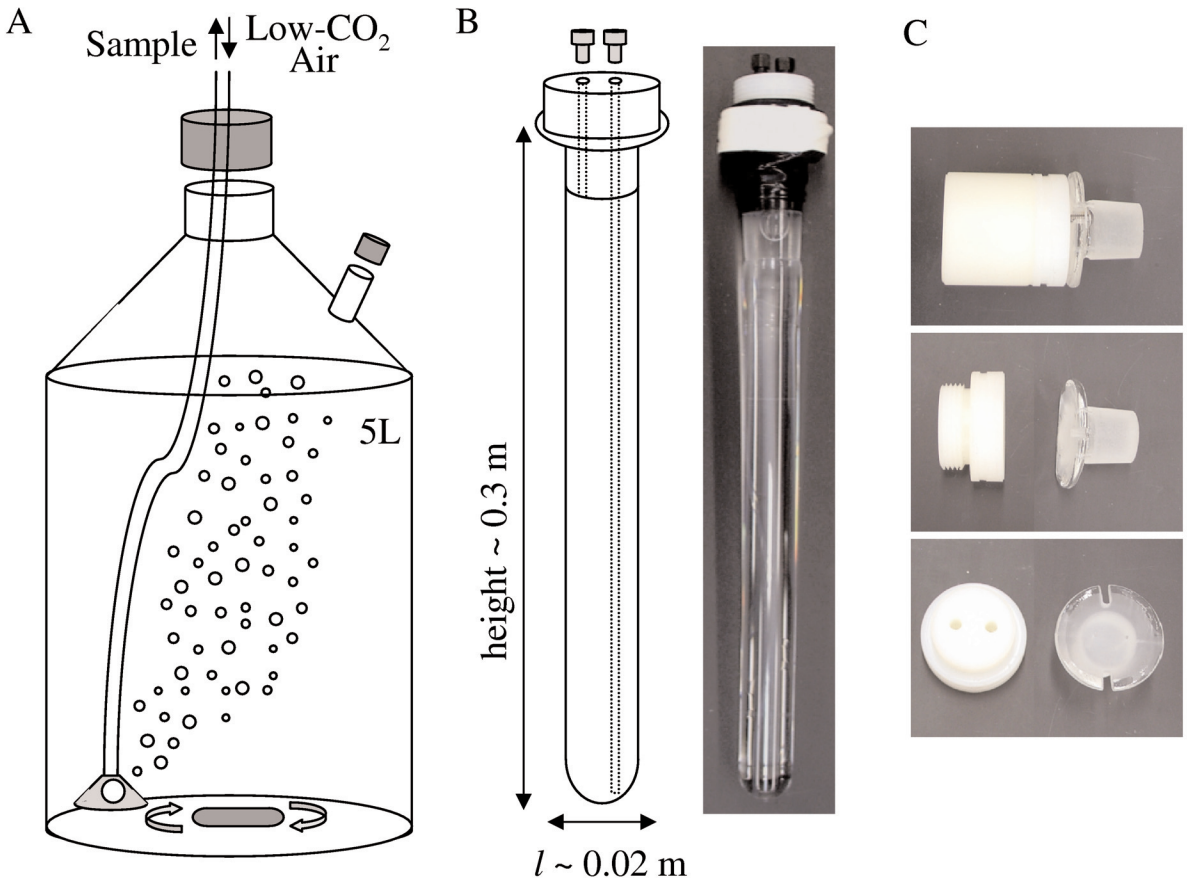

Fig. 1. Diagrams and photos of (A) sparging bottle used for sample pretreatment, (B) quartz irradiation tube, and (C) homemade nylon irradiation tube caps: side view assembled with screw cap (top panel), side view disassembled without screw cap (middle panel), and disassembled top view without screw cap (lower panel). Quartz tubes were filled from the bottom using the sample line of the sparging bottle.

9.5 × 250 mm combination AgCl pH electrode, Beckman) and was sealed with a compression cap (Chemglass) or closed off with a solid Teflon screw cap (when the electrode was not inserted). Bottles were rinsed with 10% HCl, followed by Milli-Q water and sample prior to use.

To strip DIC from seawater, samples were acidified to pH 3.0 with concentrated hydrochloric acid (Ultrex grade), converting DIC to CO_2. The acidified sample (3 to 5 L) was bubbled with low-CO_2 air (<1 ppm CO_2) at ~3.5 L min^{-1} and stirred with a magnetic stir bar for at least 10 h. The pH was then adjusted back to the original value with sodium hydroxide (50% solution). The resulting low-DIC seawater sample was then transferred pneumatically (through a short length of 1/8″ OD FEP tubing) to quartz tubes for irradiation by closing both the side port and vent to pressurize the bottle.

Irradiation conditions—For photochemical experiments, samples were irradiated in specially designed, gas-tight tubes (Fig. 1B). These tubes were made from Chemglass quartz tubing (24 mm OD and 20 mm ID) and a quartz outer joint (24/40, Chemglass). Caps were made for the tubes from solid ground glass stoppers and nylon tops (Fig. 1C). The stoppers were modified as follows: ~1.5 cm was removed from the bottom and the top was cut off and smoothed flat to ensure a good seal with the bottom of the nylon piece when attached by screws. The glass stoppers were also notched at opposite ends (Fig. 1C) to allow the stoppers to be screwed to the nylon tops. The hand machined tops had two 1/16″ diameter holes drilled near the center, running all the way through the nylon and glass stopper, which were threaded to accommodate 1/4-28 PEEK plugs (Dionex). The nylon piece was also threaded to seal tightly with an accompanying screw cap and o-ring. After being machined, the cap components were disassembled and cleaned by soaking in hexane, chloroform, acetonitrile, Milli-Q water, hydrochloric acid (10%), and Milli-Q water, consecutively. As a final step, glass stoppers were baked at 400°C for 6 h. Clean stoppers and nylon tops were then reassembled and two pieces of FEP tubing (1/16″ OD and 1/32″ ID, Cole-Parmer) were threaded through the holes. One piece of tubing was cut off at the bottom of the stopper while the other was cut long enough to reach the bottom of the quartz tube. Caps were attached to the clean quartz tubes at the ground glass fitting and then securely fastened with wire covered by black electrical tape.

To fill the quartz tubes, the sampling line of the sparging bottle was attached (using flangeless nuts and ferrules,

Upchurch) to the long piece of tubing in each quartz tube. In this configuration, quartz tubes were filled from the bottom first, minimizing turbulence and contact between the sample and the atmosphere. To further avoid CO_2 contamination, quartz tubes were overflowed with approximately three sample volumes before collecting the final sample. Once each quartz tube was filled, it was quickly capped at the outlet port (while sample flow was continued) and then at the inlet port using threaded PEEK plugs. Prior to use, tubes were cleaned by filling and soaking with HCl-acidified (pH ~3) Milli-Q water sparged with low-CO_2 air. This process was repeated several times. Low-CO_2 air (introduced through the short piece of tubing in the cap) was then used to empty the quartz tubes before refilling with sample. During filling and emptying, care was taken to maintain a positive flow of either sample or low-CO_2 air into the tube to prevent the introduction of atmospheric CO_2. After use or storage, tubes were cleaned by flushing with low-CO_2 air followed by acidified, low-DIC (~70 nmol L^{-1}) Milli-Q water in preparation for the next experiment. For each sample, three to five tubes were irradiated along with at least four dark controls (tubes wrapped in aluminum foil).

Shipboard irradiations were carried out on deck in a ~3 cm deep circulating freshwater bath (25°C to 29°C) for 6.5 h. In the laboratory, samples were irradiated for 8 h with a solar simulator consisting of five UVA-340 (Q-PANEL) and five full spectrum fluorescent light bulbs (F40T12/SR 22906, General Electric) in a rotating Milli-Q water bath (22°C to 24°C). A calibrated OL 754 scanning spectroradiometer (Optronic Laboratories) was used to quantify the photon exposure. The spectral output of the solar simulator and sunlight (noon on 1 August 2007 in Syracuse, New York) are shown in Fig. 2. Noontime sunlight was ~0.8 (290 to 340 nm) and 1.9 (340 to 400 nm) times greater than that of the solar simulator, when comparing the integrated area under the respective spectral irradiance curves in Fig. 2. Thus, the solar simulator was a good match to sunlight at $\lambda \leq 340$ nm, but the output of the solar simulator was lower than sunlight at longer wavelengths.

CDOM absorption spectra—Absorbance spectra were determined for 0.2 μm filtered samples before and after irradiation using an Agilent 8453 spectrophotometer with a 5-cm pathlength, microvolume (370 μL), flow-through quartz cell (Hellma). Milli-Q water was used as a reference and spectra were baseline corrected by adjusting the absorbance (A_λ) to zero between 700 and 800 nm (Blough et al. 1993). To quantify chromophoric DOM (CDOM), corrected absorbance values were used to calculate absorption coefficients at 330 nm:

$$a_{330} = 2.303 \times (A_{330}/l) \quad (1)$$

where l is the pathlength in meters. Each sample was analyzed in triplicate resulting in < ±2% relative standard deviation (RSD). Based on three times the standard deviation of the blank, the limit of detection for measured absorption coefficients was 0.02 m^{-1} at 330 nm. To characterize sample absorption, spectra were fit to the following exponential form (e.g., Twardowski et al. 2004):

$$a_\lambda = a_{\lambda_o} e^{-\text{slope}\,(\lambda-\lambda_o)} \quad (2)$$

where $a_{\lambda o}$ is the absorption coefficient at the reference wave-

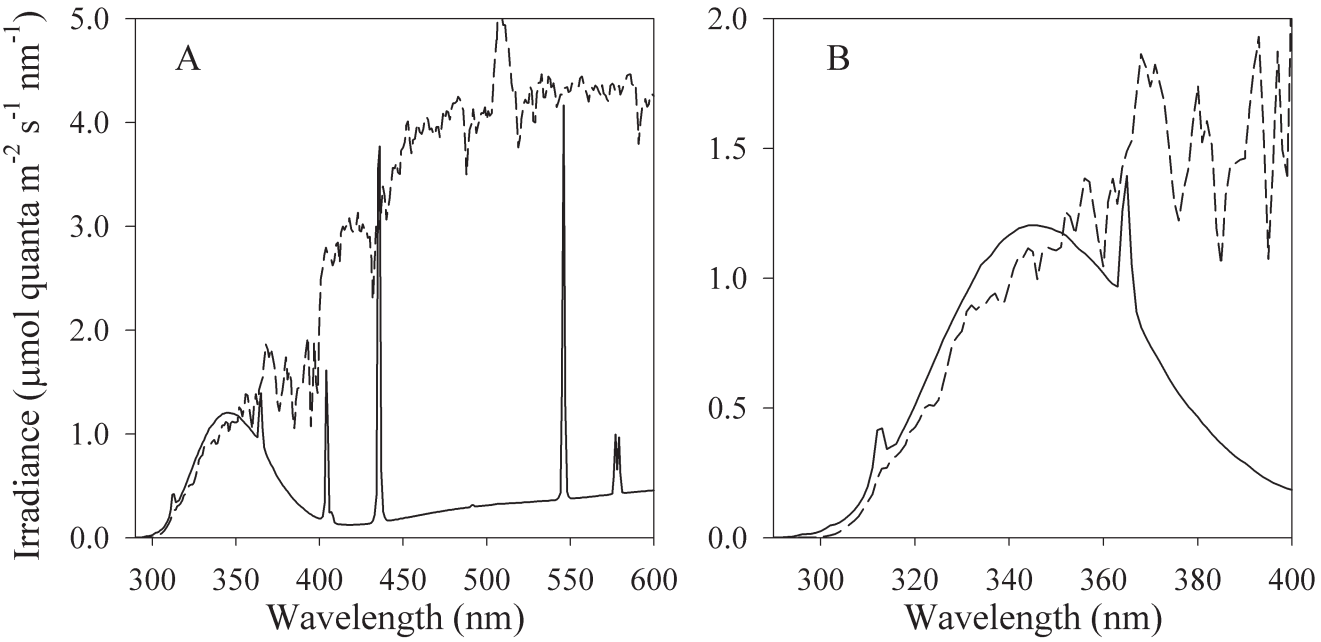

Fig. 2. (A) Full and (B) ultraviolet spectral output of the solar simulator (solid line) compared with sunlight (dashed line) measured at 1200 on 1 August 2007 on the roof on Jahn Laboratory in Syracuse, New York (43.03°N, 76.14°W). The irradiance was measured with an Optronics OL 754 scanning spectroradiometer.

length, λ_o, and slope is the spectral slope coefficient (nm^{-1}). Data were fit to a single exponential equation using SigmaPlot (SPSS). Slope coefficients were evaluated from 290 to 700 nm (λ_o = 440 nm) and 310 to 350 nm (λ_o = 330 nm).

DIC apparatus—The analysis of DIC involved acidification of the sample to convert DIC to CO_2, which is then stripped, dried, and carried to the detector in a stream of low-CO_2 carrier gas (UHP nitrogen). Unlike other systems used to measure total DIC in seawater (e.g., Salonen 1981; Kanamori 1982; Goyet and Snover 1993; Abdullah and Eek 1995; O'Sullivan and Millero 1998; Kimoto et al. 2002; Kaltin et al. 2005), our approach is unique because a closed (i.e., airtight) system is maintained throughout sample preparation and analysis to prevent atmospheric CO_2 contamination, allowing for measurement of low levels of DIC.

Details of our DIC analyzer are shown in Fig. 3. Sample injection and acid addition were accomplished using a Valco two-position, 10-port analytical injection valve (VICI). The sample loop (5 mL) was filled pneumatically by connecting the sparging bottle or quartz tube (pressurized with low-CO_2 air) to the injection valve. At the same time, the acid loop (140 μL) was filled with 20% H_3PO_4 from the acid reservoir that was sparged (to remove CO_2) and pressurized (5 psi) with low-CO_2 air. After the sample loop was overfilled with approximately three times its volume, the sample and acid were injected into the CO_2-stripping cell. Flow was forced through the bottom frit of the glass stripping cell (2.5 cm diameter and 28 cm long) using UHP nitrogen as both the injection and stripping/carrier gas. Nitrogen flow was controlled at 160 mL min^{-1} using a mass flow controller (Omega) placed directly before the LI-7000 CO_2/H_2O analyzer (LI-COR). Before reaching the detector, water vapor was removed from the gas stream with a Nafion dryer (MD-070-96F, Perma Pure) using low-CO_2 air as the counter-flow drying gas, followed by a $Mg(ClO_4)_2$ trap (fitted with a Whatman 0.1 μm PTFE, 13 mm diameter syringe filter). After analysis, the water sample was emptied from the stripping cell through a waste line. To prevent diffusion of atmospheric CO_2 into the system, stainless steel tubing was used for sample loops (type 304, 1/16" OD and 0.050" ID, Alltech) and liquid and gas lines. PEEK tubing (1/16" OD and 0.020" ID, Upchurch) was used to restrict flow through the Nafion dryer. In between injections, an ETFE shut-off valve (Upchurch) prevented sample backflow when the injector returned to the load position.

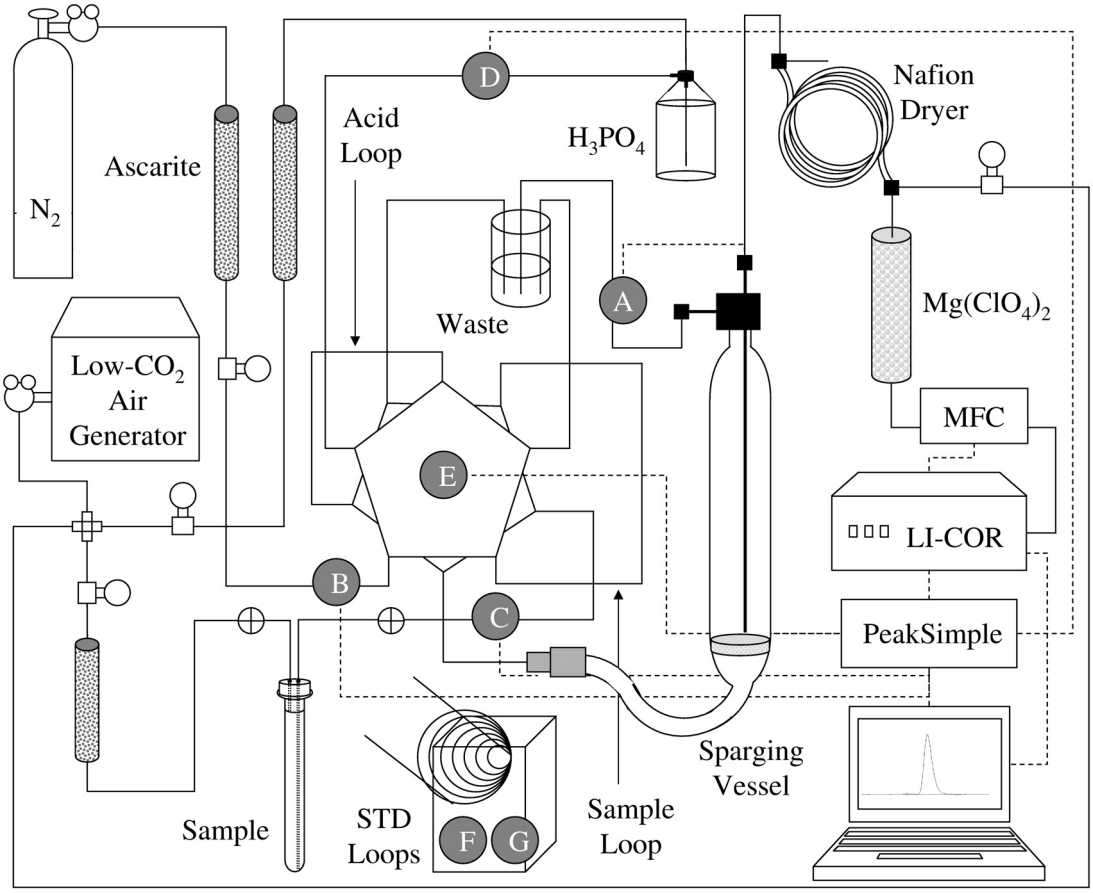

Fig. 3. Schematic of DIC analyzer. Letters correspond to the software-controlled relay of (A) sparging vessel waste line solenoid, (B) nitrogen carrier/sparge gas solenoid, (C) sample solenoid, (D) acid solenoid, (E) 10-port, 2-position Valco sample and acid valve, (F) home relay switch and (G) 14-port Valco valve for standards (STD). Dashed lines indicate electrical connections. MFC denotes mass flow controller.

The instrument was controlled using a PeakSimple Model 203 Chromatography Data System (SRI). The injection and solenoid valves (Parker Hannifin), controlled through PeakSimple software (version 3.29), were used to fill the sample and acid loops, make an injection, and empty the stripping cell. This software was also used to acquire data from the LI-COR (full scale detector setting = 10) and integrate peak areas. In addition, nitrogen flow was logged with a digital flow meter (Omega) input to the LI-7000 as an auxiliary device, using the LI-7000 PC Communications Software. Allowing for sufficient flushing of the tubing and sample loop, a single sample was analyzed in triplicate in ~20 min. For a typical experiment (i.e., 8 samples and 4 standards), the entire analysis was completed in 4 h.

Data correction—Photochemical CO_2 production was calculated from the difference in DIC between dark and light treatments. To account for absorption loss during irradiation, the geometric mean of absorption coefficients before and after light exposure ($a_{\lambda,avg}$) was used (Osburn et al. 2001). For comparative purposes, measured rates were corrected for differences in sample absorption by normalization to $a_{330,avg}$ and an overall light screening factor ($SF_{\sum\lambda}$ where $SF_\lambda = (1 - e^{-la_{\lambda,avg}})/la_{\lambda,avg}$) as described by Miller and Chin (2002). The SF was determined from 310 to 350 nm. This solar bandwidth was estimated using published apparent quantum yield spectra for CO_2 photoproduction (Johannessen and Miller 2001), which showed that maximum overlap between the solar spectrum and spectral quantum yields was at 330 nm. The resulting rates (in units of nmol C L^{-1} h^{-1} m) were then compared to evaluate differences in the photochemical efficiency of CDOM to produce CO_2.

Assessment

Calibration—Sodium carbonate standards (0, 1, 2, and 3 μmol L^{-1}) were prepared by dilution of an 85 mmol L^{-1} stock solution with low-DIC water. Sodium carbonate used for the stock solution was dried at 280°C for > 2 h (to constant weight) and stored in a dessicator over phosphorus pentoxide. The stock solution was prepared immediately before use. To prepare μmol L^{-1} standards, a calibrated volumetric flask was used to transfer 100 mL aliquots of fresh Milli-Q water to 100 mL sparging bottles (PyrexPlus© media bottles). After sparging with low-CO_2 air for at least 1 h, the stock solution was added to the low-DIC water and the bottle was quickly capped. The standard was gently mixed and pneumatically loaded into the DIC analyzer by pressurizing the headspace of the sparging bottle with low-CO_2 air. To minimize any potential exchange with the atmosphere, each standard was prepared immediately before analysis.

While low concentration (i.e., μmol L^{-1}) aqueous carbonate standards were used for routine analysis, preparation required special precautions and careful attention to avoid contamination from the atmosphere. To confirm the accuracy of these standards, a certified CO_2 gas standard and a series of stainless steel loops were used. To allow for the injection of multiple sample volumes, a 14-port Valco valve (model E6X2, VICI) was connected to the injection valve of the DIC analyzer. In this configuration, sample loop switching could be achieved while maintaining a closed system. Sample loop volumes (ranging from ~1 to 3.5 mL) were determined gravimetrically (to within ± 0.004 mL) by measuring the amount of water transferred from the filled loop to the stripping cell. A Traceable barometer (Control Company) was used to measure the atmospheric pressure and temperature during calibration.

Sensitivity and accuracy—Instrument sensitivity was inversely related to the carrier gas flow rate because slower flow resulted in a longer residence time in the detector. In our system, a flow rate of 160 mL min^{-1} was used to obtain good sensitivity [~3 V s $(\mu mol\ L)^{-1}$] while maintaining a sharp peak shape. This flow rate was selected to allow the system to recover from gas flow fluctuations following sample injection. During each analysis, the flow rate was monitored to ensure that the flow was stable (within 0.1 mL min^{-1}) while the CO_2 was carried through the detector. Over the course of a full experiment the flow rate varied by less than 0.2%. Calibration curves generated with aqueous standards were linear over the range of interest for blanks and seawater samples (0.05 to 3 μmol L^{-1}, $r^2 > 0.999$, $n = 4$). Gas loop volumes were selected to inject a comparable amount of CO_2 using a 100 ppm standard (4 to 14 nmol, $r^2 > 0.999$, $n = 4$). Linearity of the calibration was confirmed at lower concentrations by directly connecting a 150 μL loop to the system (without the 14 port Valco valve) to inject a 0.6 nmol CO_2 gas standard. A larger loop (10 mL) was used for aqueous standards, as needed (with full scale detector setting = 20), to extend the calibration up to 8 μmol L^{-1}. Excellent agreement was observed between aqueous and gas standards (Fig. 4).

Blanks—Acidified, sparged Milli-Q water served as an instrument blank and was used to flush CO_2 out of the system prior to use. After sparging 4 L acidified Milli-Q water (pH ~3) with low-CO_2 air for ~24 h, the DIC content of the resulting low-DIC water averaged 70 ± 10 nmol L^{-1} ($n = 6$). This water was also used to condition and clean the quartz tubes (as described previously). The experimental blank consisted of seawater that had been acidified, stripped of CO_2, and basified to the original pH of the sample. The DIC concentration of acidified seawater dropped quickly to about 6 μmol L^{-1} (i.e., ~99.7% DIC removal) after less than 2 h of sparging and then decreased more gradually, reaching a concentration of 130 nmol L^{-1} (i.e., > 99.99% DIC removal) after 24 h (Fig. 5). Stripped seawater samples had an average DIC concentration of 150 ± 20 nmol L^{-1} ($n = 11$). The addition of 20 mol L^{-1} sodium hydroxide (~0.3 mL) to restore sample pH generally added 300 to 800 nmol L^{-1} of DIC to the sample, because of carbonate contamination in the sodium hydroxide. Carbonate is present as a contaminant in commercially available reagent grade hydroxide. As a result, < 1 μmol L^{-1} DIC was present in the rebasified, low-DIC seawater.

Procedural blanks were analyzed to check for the diffusion of atmospheric CO_2 into the quartz tubes during filling and storage. A low-DIC Milli-Q control was transferred to quartz

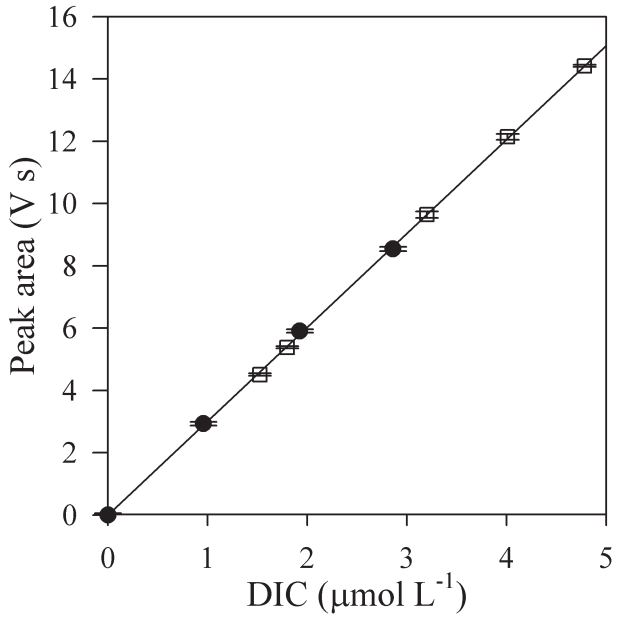

Fig. 4. Calibration curves generated with sodium carbonate standards (slope = 3.010 ± 0.020 V s [μmol $L^{-1}]^{-1}$, r^2 = 0.9995, solid circles) and a gaseous CO_2 standard (slope = 3.014 ± 0.008 V s [μmol $L^{-1}]^{-1}$, r^2 = 0.9998, open squares). The calibration curve for the aqueous standards includes a sparged Milli-Q water blank (peak area = 0.17 V s, corresponding to a concentration of approximately 60 nmol L^{-1}), which was subtracted from each standard. Error bars denote the standard deviation based on triplicate analysis of each standard.

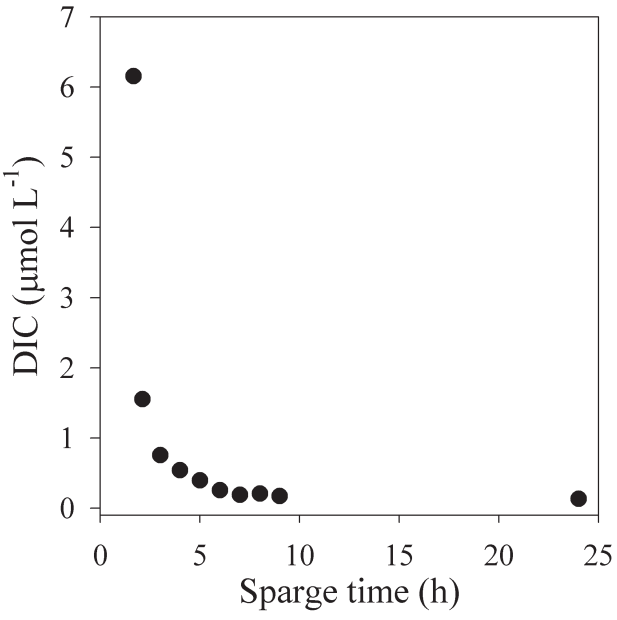

Fig. 5. Concentration of DIC in coastal seawater as a function of sparge time. Approximately 4.25 L of filtered seawater was acidified to pH 3 with concentrated hydrochloric acid and bubbled with low CO_2 air (3.5 L min^{-1}). Removal of 99.99% DIC (as CO_2) was achieved in 6 h. Each datum point represents a single injection.

tubes and analyzed within 4 h of filling. There was no significant difference in the DIC concentration of the Milli-Q control in the sparging bottle and the quartz tubes. Similarly, no significant change was observed after transferring low-DIC seawater to the quartz tubes.

Precision and detection limit—The limit of detection of the method was ~60 nmol L^{-1}, defined as the concentration corresponding to three times the standard deviation (SD) of the low-DIC seawater blank. The RSD for a 2 μmol L^{-1} standard in Milli-Q water was less than ± 1.2% (n = 3). The RSD for a 100 nmol L^{-1} standard in Milli-Q water was ± 3.4% (n = 3). However, the precision was also dependent on the agreement between multiple injections from the same tube and the reproducibility between different tubes. The precision of triplicate injections from the same tube, with a typical RSD of less than ± 2%, was comparable to injections made directly from the sparging bottle. Analysis of replicate tubes (n = 4) gave a RSD of ± 3%. The overall precision for a typical experiment in which coastal seawater collected near Block Island, Rhode Island, USA was irradiated with the solar simulator for 8 h is shown in Fig. 6. Consideration of multiple tubes (n = 4) gave an average (±SD) of 750 ± 20 nmol L^{-1} DIC in the irradiated samples (Fig. 6A). A corresponding average value of 550 ± 20 nmol L^{-1} (n = 4) was obtained for the dark control tubes (Fig. 6B). Based on the difference between light and dark samples and propagating the error, the amount of photochemical CO_2 production in this sample was 200 ± 30 nmol L^{-1} (Fig. 6C).

Analyses of natural water samples—To demonstrate the usefulness of this method, CO_2 photoproduction rates were determined for a number of different sample types. In addition to the coastal sample discussed previously, irradiations were carried out on waters from the Gulf Stream, Delaware Estuary, Cape Fear Estuary (North Carolina), and Green Lake (New York), as well as with Suwannee River fulvic acid (SRFA standard I, International Humic Substances Society). Measured CO_2 photoproduction rates ranged from 6 ± 3 nmol L^{-1} h^{-1} for the Gulf Stream to 263 ± 6 nmol L^{-1} h^{-1} for the Delaware Estuary sample (Table 1). As expected, rates increased as a function of CDOM concentration (i.e., a_{330}). Absorption coefficient-normalized rates were lowest for marine samples (40 to 50 nmol L^{-1} h^{-1} m) compared to SRFA and the terrestrially influenced estuarine sample (60 nmol L^{-1} h^{-1} m). Interestingly, the highest absorption-corrected rate (110 nmol L^{-1} h^{-1} m) was observed for Green Lake. While the error associated with some of these rates makes it difficult to evaluate specific differences, the data support the general trend that terrestrial DOM is more efficiently photomineralized than marine DOM.

A rooftop irradiation was conducted with coastal seawater (0930 to 1630 local time, 2 November 2006, Syracuse, New York, USA), resulting in the production of 240 ± 40 nmol L^{-1} CO_2 (compared with 260 ± 60 nmol L^{-1} from 8 h in the solar simulator). There was no significant difference in the loss of sample absorption observed with each light treatment. A shipboard time series was also conducted with Cape Fear Estuary

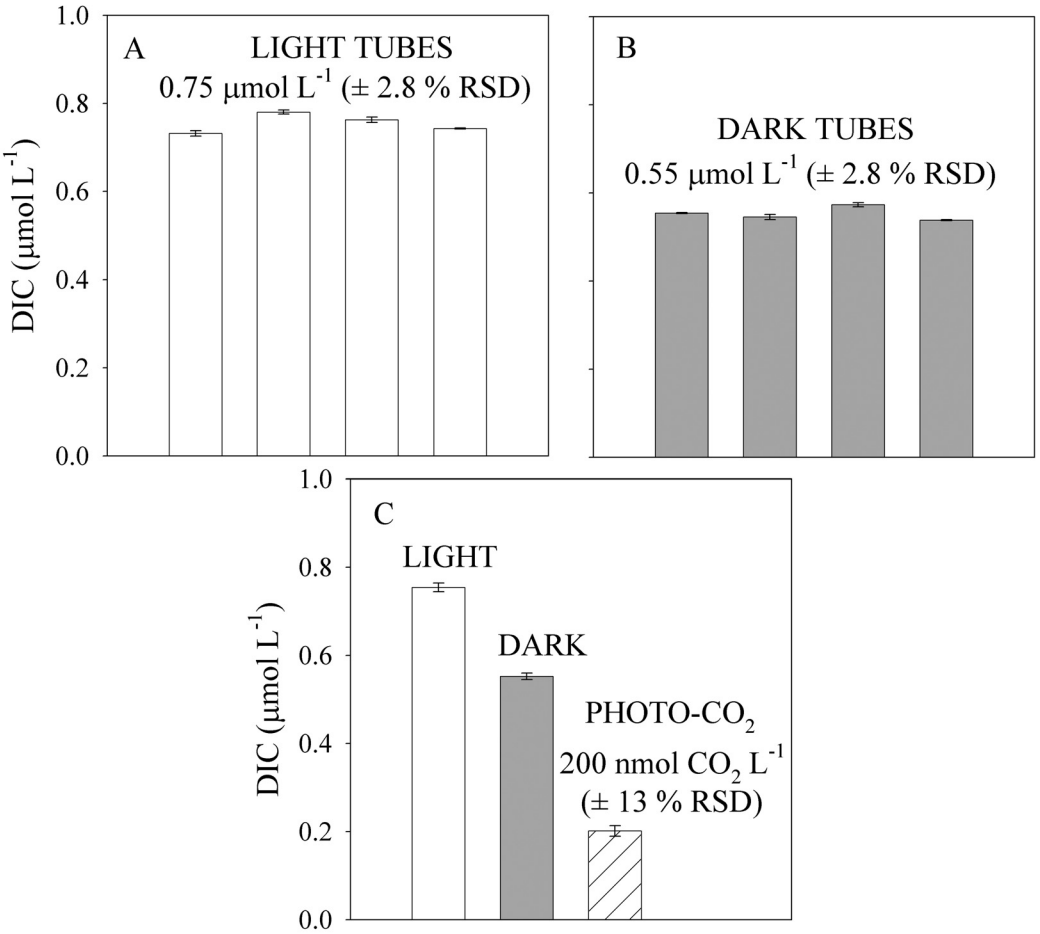

Fig. 6. Precision for an experiment in which coastal seawater (collected near Block Island, Rhode Island, USA) was irradiated in the solar simulator for 8 h. (A) Light and (B) dark quartz tubes, represented by the open and shaded bars, respectively, are presented in the order they were filled, from left to right. Replicate tubes gave good agreement, with a RSD of ±3% and no systematic concentration change was observed during filling. Error bars represent the standard deviation based on triplicate analysis of each sample. (C) Based on the difference between the average light and dark values, photochemical CO_2 production was determined with a RSD of ±13%. Error bars represent the standard deviation of the analysis of separate samples for the light and dark samples and propagation of error of the difference between these two treatments for the photoproduced CO_2.

water to investigate the relationship between light dose and CO_2 accumulation (Fig. 7). Absorption-normalized photochemical CO_2 accumulation increased linearly as a function of light dose (from 310 to 350 nm) for the first 5 h of irradiation ($r^2 > 0.99$), but production leveled off for longer irradiations. This decrease in rate may have resulted from a decrease in the efficiency of CDOM to produce CO_2 with increased light exposure (Miller and Zepp 1995) or partial shading of the quartz tubes that was not accounted for with the spectroradiometer (due to its placement on top of the ship rather than next to the water bath and quartz tubes on the aft deck).

Effect of sample pretreatment—Our sample pretreatment method involved acidification and sparging, followed by base addition to restore the sample pH. This last step was needed to minimize pH dependent differences in DOM photoreactivity (e.g., Miller and Zepp 1995; Gao and Zepp 1998; Gennings et al. 2001; Anesio and Granéli 2003). The treated water was assumed to be representative of the original sample. However, it was possible that pH adjustments irreversibly altered the DOM, potentially influencing the photochemical behavior of the sample. Differences in the chemical and physical properties of humic substances have been observed as a function of pH (Schnitzer 1980). Furthermore, at low pH, a portion of DOM may be removed due to the precipitation of humic acids. Presumably this material was redissolved when the pH was raised, but it is unclear if this processing affected DOM photoreactivity. Volatile compounds will be lost during sparging, but it is unlikely that this will significantly affect the bulk DOM since volatile organic carbon accounts for only a small fraction (<6%) of total organic carbon in marine waters (MacKinnon 1979; Gschwend et al. 1982). It is also likely that samples were concentrated slightly by evaporation during sparging (with dry air). However, this was probably offset by the sample dilution resulting from the addition of acid and base (<2 mL added to 3 L).

Table 1. Sample location, collection date, pH (of treated samples), and measured and absorption-normalized, screening factor-corrected rates for the photochemical production of CO_2 (Photo-CO_2)*†

Sample	Location	Date collected	pH	Photo-CO_2 (nmol L^{-1} h^{-1})	Photo-CO_2 normalized (nmol L^{-1} h^{-1} m)
Coastal (surface)	41.07°N 71.13°W	3 Aug 03	8.0	25 (3)	51 (7)
Gulf Stream (30 m)	35.30°N 74.36°W	29 Jul 03	8.2	6 (3)	40 (20)
Delaware (surface)	39.41°N 75.51°W	29 Jun 02	7.9	263 (6)	63 (1)
Green Lake‡ (surface)	43.05°N 75.97°W	5 Nov 05	8.1	41 (4)	110 (10)
SRFA§	NA#	NA	6.1	162 (5)	59 (2)
SRFA§ (untreated)	NA#	NA		110 (10)	63 (7)

*All samples were irradiated for 8 h in the solar simulator. Based on a daily photon exposure of ~1 mol quanta m^{-2} d^{-1} from 310 to 350 nm, 8 h of solar simulator light is roughly equivalent to 1 day of summer sunlight at ~40°N (in terms of CO_2 photoproduction).
†Values in parentheses denote the standard deviation based on propagation of error from triplicate analyses of replicate light and dark samples (Photo-CO_2).
‡Green Lake is a pristine, meromictic lake located in Fayetteville, New York, USA.
§SRFA is Suwannee River fulvic acid. The untreated sample was not pH adjusted and sparged.
#NA is not applicable.

These effects were examined by analyzing highly productive samples with and without pH adjustment and sparging. Whereas the effect of pretreatment on CDOM spectra were difficult to evaluate, small changes were easily observed in absorption coefficients and spectral slopes (Table 2). Typically, an overall increase of < 20% was seen in the absorption coefficient at 330 nm. For example, when the pH of coastal seawater was adjusted, an overall increase of 0.05 ± 0.01 m^{-1} was observed (i.e., from 0.506 ± 0.007 m^{-1} to 0.555 ± 0.007 m^{-1}, Fig. 8). Small changes were also observed in the spectral slope following pH adjustment, but a consistent trend was not seen for all samples (Table 2). Control experiments using Milli-Q water showed that pretreatment had no appreciable effect on absorption at wavelengths > 290 nm. This suggests that the observed increase in absorption and associated changes in spectral slope were likely due to pH-induced changes in the DOM rather than direct absorption by contaminants added with the acid and base. However, other more complicated processes may be involved. For example, metal-DOM complexes could be responsible for changes in sample absorption (or photochemistry) if metal concentrations (e.g., iron) increased as a result of pretreatment. The use of sodium borate instead of sodium hydroxide gave a similar absorption change (but resulted in slightly higher background DIC; data not shown).

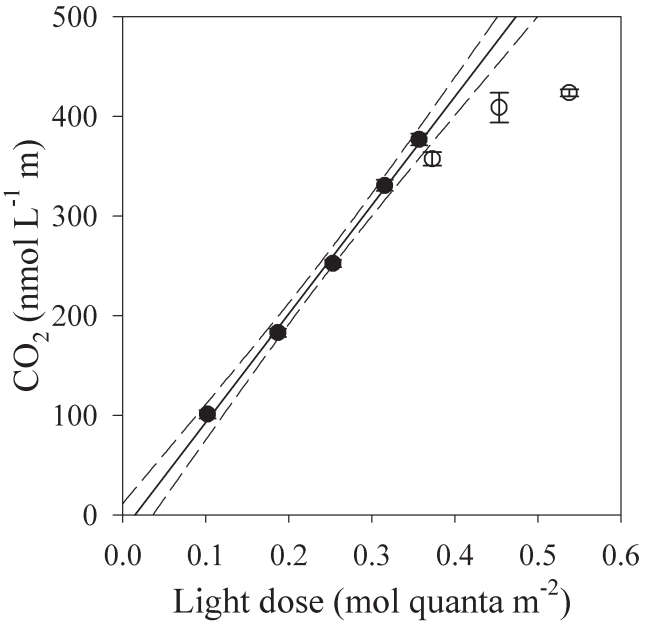

Fig. 7. CO_2 photoproduction as a function of light dose in a sample from the Cape Fear Estuary (salinity = 14, pH = 7.9, a_{330} = 36 m^{-1}). This shipboard time series was carried out from 930 to 1245 local time on 24 July 2003, with samples analyzed every 30 to 45 min. Each datum point represents an individual tube (i.e., DIC in a single light tube minus the average of four dark tubes). All analyses were done in triplicate, and error bars represent the corresponding standard deviation. Where not visible, error bars are contained within the symbols. Rates were corrected for inner filter effects by normalization to $a_{330,avg}$ and $SF_{\Sigma 310\text{-}350}$. The light dose (from 310 to 350 nm) was measured with an Optronics OL 754 scanning spectroradiometer, which was located on the top deck of the ship. The solid line shows the best-fit linear regression (r^2 = 0.997) of the first five time points (filled circles) excluding tubes exposed to higher light doses (open circles). The dashed lines indicate the 95% confidence interval of the regression line.

Potential artifacts with our method were investigated by comparing CO_2 photoproduction rates in an untreated sample with a sample that was acidified, sparged, and basified to its original pH. To measure photoproduction rates in an untreated sample, it must have a reasonably low background DIC and/or high DOM content. Suwannee River fulvic acid (~1 mg organic carbon L^{-1}) was therefore used for the comparative study. While this sample is not necessarily representative of marine waters, it provided evidence that pretreatment did not result in significant sample modification. No difference was observed between CO_2 photoproduction rates in untreated (63 ± 7 nmol DIC L^{-1} h^{-1} m) and treated (59 ± 2 nmol DIC L^{-1} h^{-1} m) SRFA samples. Light control experiments with Milli-Q water showed no CO_2 production.

To further investigate the effect of sample pretreatment on CO_2 photoproduction rates, we carried out a series of experiments

Table 2. Sample pH, absorption coefficient at 330 nm (a_{330}), and spectral slope from 290 to 700 nm (λ_0 = 440 nm) and 310 to 350 nm (λ_0 = 330 nm) for untreated and treated (i.e., pH adjusted and sparged) samples*

Sample	pH		a_{330} (m^{-1})		$Slope_{290\text{-}700}$ (nm^{-1})		$Slope_{310\text{-}350}$ (nm^{-1})	
	Untreated	Treated	Untreated	Treated	Untreated	Treated	Untreated	Treated
Coastal† (surface)	8.1	8.0	0.506 (0.007)	0.555 (0.007)	0.0175	0.0181	0.0202	0.0202
Gulf Stream (30 m)	8.3	8.2	0.138 (0.001)	0.158 (0.001)	0.0161	0.0171	0.0183	0.0182
Delaware (surface)	7.8	7.9	4.386 (0.002)	4.908 (0.002)	0.0189	0.0180	0.0188	0.0179
Green Lake (surface)	7.7	8.1	0.341 (0.001)	0.510 (0.009)	0.0194	0.0211	0.0285	0.0260
SRFA‡	6.5	6.1	2.667 (0.005)	3.133 (0.004)	0.0173	0.0158	0.0143	0.0128
SRFA‡ (untreated)	5.6		1.915 (0.004)		0.0176		0.0143	

*Values in parentheses denote the standard deviation based on triplicate analyses of replicate samples.
†The coastal sample was collected near Block Island, Rhode Island, USA.
‡SRFA is Suwannee River fulvic acid.

in which our results were directly compared with those obtained with a newly developed, independent method (Zafiriou et al. 2003*b*). In the approach of Zafiriou et al. (2003*b*), natural $DI^{12}C$ in seawater was exchanged with $^{13}CO_2$ before irradiation. As with our DIC removal procedure, isotopic exchange reduced background $DI^{12}C$ so lower levels of photoproduced $DI^{12}C$ could be quantified. However, there was no acid or base addition and no bubbling, thereby minimizing sample perturbation (only $^{13}CO_2$ was added). Comparing this technique to our method, it was observed that rates measured in the same coastal sample agreed within the reported precision (Table 3). Although not statistically different, our rates were slightly larger than those measured using the isotopic exchange method. Given the higher CDOM absorption of our samples (~10% at 330 nm), this is not surprising since photoreactivity is largely controlled by CDOM absorbance (for review see Mopper and Kieber 2000). Yet, it is important to note that the pH-induced absorption changes were not significant relative to the precision of the CO_2 photoproduction measurements.

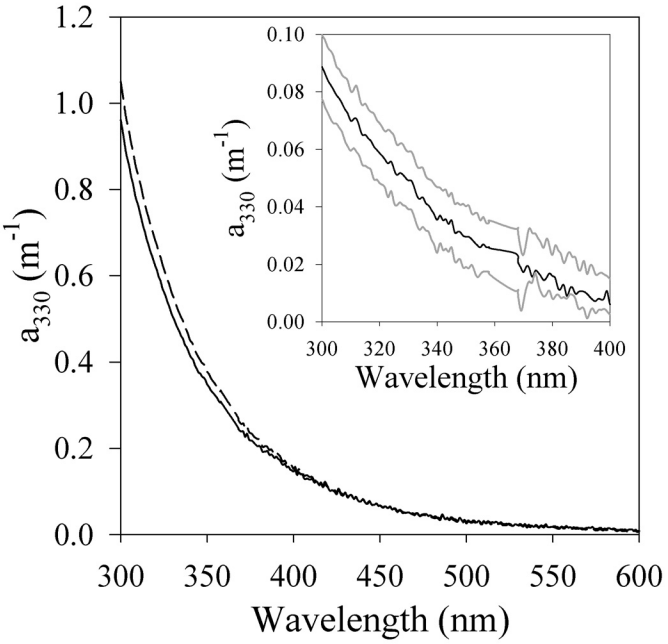

Fig. 8. Effect of pretreatment (i.e., pH adjustment and sparging) on the absorption spectrum of coastal seawater (collected near Block Island, Rhode Island, USA). As a result of pretreatment (dashed line, pH = 8.0), the sample absorption increased at wavelengths below 400 nm compared with the original, untreated sample (solid line, pH = 8.1). Insert shows the difference spectrum (i.e., spectra of original sample subtracted from spectra after treatment) with the associated error spectra (± standard deviation, gray lines). Absorption coefficients were calculated from baseline-corrected absorbance spectra measured with an Agilent 8453 spectrophotometer (5-cm pathlength).

Comparison with published data—It is difficult to directly compare different samples and studies, since published rates were not corrected for screening or normalized to the photon exposure. The CO_2 photoproduction rate (263 nmol L^{-1} h^{-1}) measured in our Delaware Estuary sample (salinity = 7, pH = 8.0, a_{350} = 3.0 m^{-1}) was more than a factor of two lower than that reported for a comparable sample (salinity = 20, pH = 8.2, a_{350} = 2.3 m^{-1}) from the Mississippi River Plume (700 nmol L^{-1} h^{-1}, Miller and Zepp 1995). CO_2 photoproduction in our Green Lake sample (pH = 8, a_{280} = 1.2 m^{-1}) was the same as the lowest rate reported (42 nmol L^{-1} h^{-1}) in the lake study of Bertilsson and Tranvik (2000) for Äspuss Lake (pH = 8.8, a_{280} = 85.8 m^{-1}). We are the first to report a CO_2 photoproduction rate as low as 6 nmol L^{-1} h^{-1} (for the Gulf Stream). To the best of our knowledge, surface rates of CO_2 photoproduction have not been previously reported for coastal and open ocean waters. Investigations of CO_2 photoproduction in seawater have been limited to apparent quantum yield (AQY) spectra (Johannessen and Miller 2001; Bélanger et al. 2006; Skalski 2006; Johannessen et al. 2007).

In these studies, AQY (i.e., moles of DIC formed divided by moles of photons absorbed by CDOM) were determined using a multispectral polychromatic approach in which CO_2 photoproduction rates measured under a series of long-pass cutoff filters were modeled to describe AQY as a function of wavelength (e.g., Johannessen and Miller 2001). AQY spectra can be used to calculate rates as a function of solar irradiance (for waters with a known absorption spectrum), thereby predicting CO_2 production

Table 3. CO_2 photoproduction rates measured using our DIC removal method, the isotopic exchange method of Zafiriou et al. (2003*b*), and predicted from the AQY spectra of Johannessen and Miller (2001)*

Sample	Salinity	Irr. time (h)	Removal method	Photochemical CO_2 production		
				Isotope exchange method (nmol L^{-1} h^{-1})	Ocean AQY Prediction (nmol L^{-1} h^{-1})	Coastal AQY Prediction (nmol L^{-1} h^{-1})
Gulf Stream	36	8	6 (3)		3	1
Coastal	32	8	25 (2)			
Coastal	32	21.6	†31 (4)			
Coastal	32	37.5	†29.4 (0.7)	†25 (7)		
Coastal	32	37.5		†24 (5)		
Coastal	32	47.0	†24 (4)	†22 (3)		
Coastal	32	AVG	28 ± 3	24 ± 1	17	6

*Rates reported here are for measured production (i.e., not normalized to sample absorption) resulting from irradiation in the solar simulator. Values in parentheses denote the standard deviation based on propagation of error from replicate samples ($n \geq 4$) and analyses.
†Rates used to determine the average rate for the coastal sample (collected near Block Island, Rhode Island, USA). For the average rate, the error denotes standard deviation of the three rates.

in a given sample. For comparative purposes, we used the pooled AQY spectra for DIC photoproduction in coastal (salinity = 31 to 35) and open ocean (salinity > 35) waters (Johannessen and Miller 2001) to calculate predicted CO_2 photoproduction rates for our coastal and open ocean samples.

Rates of photochemical CO_2 production were calculated from the pooled AQY spectra, CDOM absorption spectra, and spectral irradiance integrated over the wavelength range of 290 to 480 nm according to the following equation:

$$\frac{dCO_2}{dt} = \int AQY(\lambda)\, E_0(\lambda) \left(1 - e^{-a(\lambda)l}\right) \left(\frac{S}{V}\right) d\lambda \qquad (3)$$

where $E_0(\lambda)$ is the incident spectral irradiance (mol quanta m^{-2} nm^{-1}) measured with the spectroradiometer and integrated over the time during which each sample was irradiated. The surface area to volume ratio (S/V) of the irradiation vessel was estimated as $4(\pi l)^{-1}$. These calculations enabled a valid comparison between our directly measured rates and those predicted from AQY spectra. The value (3 nmol L^{-1} h^{-1}) predicted for CO_2 photoproduction from the open ocean AQY (AQY = $e^{-(5.53+0.00914[\lambda-290])}$) of Johannessen and Miller (2001) is in good agreement with our measured production in the Gulf Stream (Table 3). However, the predicted production in the coastal sample (6 nmol L^{-1} h^{-1}), based on the coastal AQY (AQY = $e^{-(6.36+0.0140[\lambda-290])}$) of Johannessen and Miller (2001), underestimated our measured production (28 nmol L^{-1} h^{-1}) by almost a factor of five. Applying the open ocean AQY to the coastal sample yielded better agreement, but the measured value was still higher than the predicted value (17 nmol L^{-1} h^{-1}). This suggests that the coastal AQY should be higher than the open ocean AQY (in disagreement with the findings of Johannessen and Miller [2001]) or that classification of water type by salinity alone is insufficient to predict CO_2 photoproduction (i.e., spectral AQYs cannot be extrapolated to all waters). More recent AQY work supports the general trend of higher AQY in terrestrial influenced freshwaters compared to marine waters (Bélanger et al. 2006; Skalski 2006).

Discussion

Whereas the techniques used in our experiments (i.e., sample pretreatment and DIC analyzer) are not different from those of Johannessen and Miller (2001), our system offers several improvements. Specifically, maintenance of a closed system between the sample, quartz tubes, and DIC analyzer resulted in a lower background, thereby improving the precision, lowering the limit of detection, and allowing for shorter irradiation times in photochemical experiments. Furthermore, the use of low concentration DIC standards that bracketed sample concentrations allowed for better confirmation of the system's accuracy. These enhancements made it possible to precisely measure sub-μmol L^{-1} differences in DIC concentrations. The development, testing, and authentication of the DIC system and procedure described here illustrates the usefulness of this method for the determination of CO_2 photoproduction in natural waters. Of particular importance is the applicability of this method to coastal and open ocean waters, for which we present the first directly measured rates. By studying photochemical CO_2 production in a variety of marine waters with different optical properties, a more accurate global estimate can be established for this potentially significant carbon flux.

CO_2 photoproduction measured in our Gulf Stream sample served to confirm the published open ocean AQY of Johannessen and Miller (2001). However, our coastal results suggest that these waters can produce CO_2 more efficiently than open ocean waters. More work is needed to confirm these findings and evaluate differences between waters. Our DIC analyzer provides a straightforward, convenient method for CO_2 photoproduction studies at sea and in the laboratory. In addition to measuring production rates for different waters, this technique

can be used to investigate the effect of various properties (i.e., pH, ionic strength, DOM character, etc) on the photochemical mineralization of DOM.

Comments and recommendations

Method precision is highly dependent on the quality of the hand-machined quartz tube caps. A tight fit between the inserted tubing and the drilled holes is crucial to ensure proper sealing. This requires careful drilling, tubing selection (i.e., outer diameter), and assembly (so tubing is not stretched during threading). Before initial use, the integrity of the quartz tubes must be confirmed by checking for leakage (i.e., contamination by atmospheric CO_2) during storage and analysis. Quartz tubes that systematically gave high DIC values and/or poor precision were taken apart and reassembled (or discarded if the problem could not be corrected). As work progressed, the best tubes were identified and used for future experiments to ensure good precision. Tubes were thoroughly flushed with acidified, low-DIC Milli-Q water and sample before filling. While time consuming, this process prevented contamination from the previous sample without opening tubes to the atmosphere during cleaning. Modifications to the current tube design are currently being considered to address these concerns and speed up the tube flushing/filling procedure. It should be noted that we found it necessary to use modified solid glass stoppers to seal the quartz tubes instead of plastic (e.g., Teflon) stoppers. The use of plastic resulted in high DIC blanks due to the diffusion of CO_2 out of the plastic and between the stopper and tube.

The DIC analyzer can be used to determine total DIC concentrations by making a few simple adjustments (i.e., 60 μL sample loop, nitrogen carrier gas flow rate = 300 mL min^{-1}, full scale detector setting = 150) and calibrating the system with 1.0 to 3.0 mmol L^{-1} sodium carbonate standards (in freshly collected Milli-Q water). The RSD of a 2 mmol L^{-1} seawater sample was < ±0.2%.

References

Abdullah, M. I., and E. Eek. 1995. Automated method for the determination of total CO_2 in natural waters. Water Res. 29:1231-1234.

Anesio, A. M., and W. Granéli. 2003. Increased photoreactivity of DOC by acidification: Implications for the carbon cycle in humic lakes. Limnol. Oceanogr. 48:735-744.

Bélanger, S., H. Xi, N. Krotkov, P. Larouche, W. F. Vincent, and M. Babin. 2006. Photomineralization of terrigenous dissolved organic matter in Arctic coastal waters from 1979 to 2003: Interannual variability and implications of climate change. Global Biogeochem. Cycles 20, GB4005, doi:10.1029/2006GB002708.

Bertilsson, S., and L. J. Tranvik. 2000. Photochemical transformation of dissolved organic matter in lakes. Limnol. Oceanogr. 45:753-762.

Blough, N. V., O. C. Zafiriou, and J. Bonilla. 1993. Optical absorption spectra of waters from the Orinoco River Outflow: terrestrial input of colored organic matter to the Caribbean. J. Geophys. Res. 98:2271-2278.

Conrad, R., W. Seiler, G. Bunse, and H. Giehl. 1982. Carbon monoxide in seawater (Atlantic Ocean). J. Geophys. Res. 87:8839-8852.

Gao, H., and R. G. Zepp. 1998. Factors influencing photoreactions of dissolved organic matter in a coastal river of the Southeastern United States. Environ. Sci. Technol. 32:2940-2946.

Gennings, C., L. A. Molot, and P. J. Dillon. 2001. Enhanced photochemical loss of organic carbon in acidic waters. Biogeochemistry 52:339-354.

Goyet, C., and S. D. Hacker. 1992. Procedure for calibration of a coulometric system used for total inorganic carbon measurements of seawater. Mar. Chem. 38:37-51.

——— and A. K. Snover. 1993. High-accuracy measurements of total dissolved inorganic carbon in the ocean: comparison of alternate detection methods. Mar. Chem. 44:235-242.

Granéli, W., M. Lindell, B. M. de Faria, and F. de Assis Esteves. 1998. Photoproduction of dissolved inorganic carbon in temperate and tropical lakes - dependence on wavelength band and dissolved organic carbon concentration. Biogeochemistry 43:175-195.

———, M. Lindell, and L. Tranvik. 1996. Photo-oxidative production of dissolved inorganic carbon in lakes of different humic content. Limnol. Oceanogr. 41:698-706.

Gschwend, P. M., O. C. Zafiriou, R. F. C. Mantoura, R. P. Schwarzenbach, and R. B. Gagosian. 1982. Volatile organic compounds at a coastal site. 1. Seasonal variations. Environ. Sci. Technol. 16:31-38.

Hedges, J. I., R. G. Keil, and R. Benner. 1997. What happens to terrestrial organic matter in the ocean? Org. Geochem. 27:195-212.

Johannessen, S. C. 2000. A photochemical sink for dissolved organic carbon in the ocean. Ph.D. thesis. Dalhousie University.

———, and W. L. Miller. 2001. Quantum yield for the photochemical production of dissolved inorganic carbon in seawater. Mar. Chem. 76:271-283.

———, M. A. Peña, and M. L. Quenneville. 2007. Photochemical production of carbon dioxide during a coastal phytoplankton bloom. Est. Coast. Shelf Sci. 73:236-242.

Johnson, K. M., K. D. Wills, D. B. Butler, W. K. Johnson, and C. S. Wong. 1993. Coulometric total carbon dioxide analysis for marine studies: maximizing the performance of an automated gas extraction system and coulometric detector. Mar. Chem. 44:167-187.

Kaltin, S., C. Haraldsson, and L. G. Anderson. 2005. A rapid method for determination of total dissolved inorganic carbon in seawater with high accuracy and precision. Mar. Chem. 96:53-60.

Kanamori, S. 1982. Shipboard calibration of an infrared

absorption gas analyser for total carbon dioxide determination in sea water. J. Oceanogr. Soc. Japan 38:131-136.

Kieber, D. J., E. M. White, and K. Mopper. 2003. Photochemical formation of dissolved inorganic carbon in seawater: analytical aspects and recent cruise results. Preprints of Extended Abstracts presented at the ACS National Meeting, American Chemical Society, Division of Environmental Chemistry 43:357-360.

Kimoto, H., K. Nozaki, S. Kudo, K. Kato, A. Negishi, and H. Kayanne. 2002. Achieving high time-resolution with a new flow-through type analyzer for total inorganic carbon in seawater. Anal. Sci. 18:247-253.

Ma, X. D., and S. A. Green. 2004. Photochemical transformation of dissolved organic carbon in Lake Superior - an in-situ experiment. J. Great Lakes Res. 30:97-112.

MacKinnon, M. D. 1979. The measurement of the volatile organic fraction of the TOC in seawater. Mar. Chem. 8:143-162.

Miles, C. J., and P. L. Brezonik. 1981. Oxygen consumption in humic-colored waters by a photochemical ferrous-ferric catalytic cycle. Environ. Sci. Technol. 15:1089-1095.

Miller, P. L., and Y.-P. Chin. 2002. Photoinduced degradation of carbaryl in a wetland surface water. J. Agric. Food Chem. 50:6758-6765.

Miller, W. L., and R. G. Zepp. 1995. Photochemical production of dissolved inorganic carbon from terrestrial organic matter: significance to the oceanic organic carbon cycle. Geophys. Res. Lett. 22:417-420.

Moore, R. J. 1999. Photochemical degradation of coloured dissolved organic matter in two Nova Scotian lakes. M.S. thesis. Dalhousie University.

Mopper, K., and D. J. Kieber. 2000. Marine photochemistry and its impact on carbon cycling, p. 101-129. *In* S. de Mora, S. Demers and M. Vernet [eds.], Effects of UV radiation in the marine environment. Cambridge Environmental Chemistry Series Univ. Press.

Moran, M. A., and R. G. Zepp. 1997. Role of photoreactions in the formation of biologically labile compounds from dissolved organic matter. Limnol. Oceanogr. 42:1307-1316.

O'Sullivan, D. W., and F. J. Millero. 1998. Continual measurement of the total inorganic carbon in surface seawater. Mar. Chem. 60:75-83.

Osburn, C. L., H. E. Zagarese, D. P. Morris, B. R. Hargreaves, and W. E. Cravero. 2001. Calculation of spectral weighting functions for the solar photobleaching of chromophoric dissolved organic matter in temperate lakes. Limnol. Oceanogr. 46:1455-1467.

Robinson, C., and P. J. L. Williams. 1991. Development and assessment of an analytical system for the accurate and continual measurement of total dissolved inorganic carbon. Mar. Chem. 34:157-175.

Salonen, K. 1981. Rapid and precise determination of total inorganic carbon and some gases in aqueous solutions. Wat. Res. 15:403-406.

——— and A. Vähätalo. 1994. Photochemical mineralization of dissolved organic matter in Lake Skjervatjern. Environ. Int. 20:307-312.

Schnitzer, M. 1980. Effect of low pH on the chemical structure and reactions of humic substances, p. 203-222. *In* T. C. Hutchinson and M. Havas [eds.], Effects of acid precipitation on terrestrial ecosystems. NATO Conference Series I: Ecology. Plenum Press.

Skalski, M. 2006. Seasonal estimates of photochemical production of dissolved inorganic carbon from terrestrial organic matter in an Atlantic Canada Coastal Zone Estuary. M.S. thesis. Dalhousie University.

Stubbins, A., G. Uher, C. S. Law, K. Mopper, C. Robinson, and R. C. Upstill-Goddard. 2006. Open-ocean carbon monoxide photoproduction. Deep-Sea Res. II 53:1695-1705.

Twardowski, M. S., E. Boss, J. M. Sullivan, and P. L. Donaghay. 2004. Modeling the spectral shape of absorption by chromophoric dissolved organic matter. Mar. Chem. 89:69-88.

Vähätalo, A. V., M. Salkinoja-Salonen, P. Taalas, and K. Salonen. 2000. Spectrum of the quantum yield for photochemical mineralization of dissolved organic carbon in a humic lake. Limnol. Oceanogr. 45:664-676.

Valentine, R. L., and R. G. Zepp. 1993. Formation of carbon monoxide from the photodegradation of terrestrial dissolved organic carbon in natural waters. Environ. Sci. Technol. 27:409-412.

White, E. M., D. J. Kieber, J. Sherrard, A. P. Stubbins, K. Mopper, W. Miller, and D. S. Benati. 2003. Photochemical formation of dissolved inorganic carbon in the Delaware Estuary. Preprints of Extended Abstracts presented at the ACS National Meeting, American Chemical Society, Division of Environmental Chemistry 43:361-364.

Zafiriou, O. C., S. S. Andrews, and W. Wang. 2003*a*. Concordant estimates of ocean carbon monoxide source and sink processes in the Pacific yield a balanced global "blue-water" CO budget. Global Biogeochem. Cycles. 17:1015, doi:10.1029/2001GB001638.

———, W. Wang, K. Takeda, C. G. Johnson, R. G. Najjar, E. Franks, and T. F. Dorsey, Jr. 2003*b*. Carbon dioxide as a product of CDOM photolysis: how to measure a major new carbon cycle budget term? Preprints of Extended Abstracts presented at the ACS National Meeting, American Chemical Society, Division of Environmental Chemistry 43:351-356.

Submitted 2 December 2007
Revised 26 June 2008
Accepted 4 August 2008